# Observations of sausage modes in magnetic pores

R.J. Morton[1], R. Erdélyi[1], D.B. Jess[2] and M. Mathioudakis[2]

[1]*Solar Physics and Space Plasma Research Centre (SP²RC), University of Sheffield, Hicks Building, Hounsfield Road, Sheffield S3 7RH, UK;*
[2]*Astrophysics Research Center, School of Mathematics and Physics, Queen's University, Belfast BT7 1NN, UK*

[R.J.Morton,Robertus]@sheffield.ac.uk

## ABSTRACT

We present here evidence for the observation of the magneto-hydrodynamic (MHD) sausage modes in magnetic pores in the solar photosphere. Further evidence for the omnipresent nature of acoustic global modes is also found. The empirical decomposition method of wave analysis is used to identify the oscillations detected through a 4170 Å 'blue continuum' filter observed with the Rapid Oscillations in the Solar Atmosphere (ROSA) instrument. Out of phase, periodic behavior in pore size and intensity is used as an indicator of the presence of magneto-acoustic sausage oscillations. Multiple signatures of the magneto-acoustic sausage mode are found in a number of pores. The periods range from as short as 30 s up to 450 s. A number of the magneto-acoustic sausage mode oscillations found have periods of 3 and 5 minutes, similar to the acoustic global modes of the solar interior. It is proposed that these global oscillations could be the driver of the sausage type magneto-acoustic MHD wave modes in pores.

*Subject headings:* plasmas - Sun: photosphere - waves

## 1. Introduction

The solar atmosphere is a highly dynamic magnetised plasma containing a large array of distinct structures that are defined by magnetic inhomogeneities. Each of these structures are able to support a wide variety of oscillatory magneto-hydrodynamic (MHD) modes. Over the last 50 years there has been a steady increase in the number of observations of oscillatory phenomena in the solar atmosphere being reported (for latest reviews see, e.g. Banerjee et al., 2007; De Moortel, 2009; Zaqarashvili & Erdélyi, 2009; Mathioudakis et al., 2010) showing waves and oscillations are ubiquitous in the solar atmosphere. The increase in observations coincides with the continuous

improvement of space and ground-based observing technology allowing unprecedented spatial and temporal resolution.

This high spatial and temporal resolution permits detailed investigation of some of the Sun's smallest, currently detectable magnetic features. One such feature are magnetic pores that have diameters ranging from $1 - 6$ Mm. The pores are regions of intense magnetic fields ($\sim$ 1700 G) first visible in the photosphere and expanding as they reach chromospheric heights. Pores show highly dynamic behavior due to a constant buffeting from the convective motion of granules at the photospheric level (Sobotka, 2003; Sankarasubramanian & Rimmele, 2003). There has recently been observations of photospheric structures experiencing a vortex style motion which could act as a driver for a wide variety of waves and oscillations (Bonet et al., 2008). These waves and oscillations may be able to propagate upwards through the various layers in the lower solar atmosphere along the length of the pore, which itself acts as an MHD waveguide. The majority of these waves will be reflected at the transition region due to the steep gradients in sound or Alfvén speeds, the minority, however, will make it into the corona. The transmitted portion of the waves may be relevant for MHD wave heating or magneto-seismology of the solar corona (see, e.g. Klimchuk, 2006; Taroyan & Erdélyi, 2009). One of the exciting new discoveries associated with magnetic elements in the lower solar atmosphere is evidence for torsional Alfvén waves (Jess et al., 2009) which has, historically, been difficult to detect. Would pores be able to support the other magneto-acoustic modes? If yes, would these modes be sausage or kink? We answer these questions in the current Letter.

The nature of MHD waves in sunspots and pores has been extensively investigated, where the sunspots are modelled as thin, gravitationally stratified flux tubes (Roberts & Webb, 1978; Roberts, 1981; Roberts, 1992). The seminal theory of Edwin & Roberts (1983) describing waves in a straight, magnetic cylinder, which has been applied extensively to coronal oscillations, was also derived for photospheric conditions. This last aspect is somewhat neglected and has only received limited attention although offering equally rich physics and opportunity for solar magneto-seismology as its coronal application. Dispersion diagrams for the photosphere (see, e.g. Edwin & Roberts, 1983; Erdélyi & Fedun, 2010) show clearly the nature of the waves supported by a photospheric waveguide. Perhaps more relevant to waves in pores are the dispersion diagrams presented in Evans & Roberts (1990).

The sausage oscillation is thought to be driven by the granular buffeting and the vortex motion, so pores are a good candidate for the observation of this oscillatory mode because of their compact structure. A further postulated driver maybe $p$-modes or magneto-acoustic waves which propagate within the solar interior (Dorotovič et al., 2008). The main feature of the sausage mode is the periodic fluctuation of the cross-sectional area of the wave guide (see, e.g. Edwin & Roberts, 1983 for cylindrical and Erdélyi & Morton, 2009 for elliptical wave guides). Neither Alfvén nor

kink oscillations would show evidence of perturbations of the cross-section of the waveguide. The change in the area of the cross-section caused by the sausage motion is also associated with periodic fluctuations in density and temperature within the waveguide.

Up until recently it has been almost impossible to find evidence for periodic change in cross-sections of waveguides (in any layer of the solar atmosphere), which indicates the presence of sausage oscillations. This is due to the limitations of the spatial resolution of many observing instruments. A number of earlier observations have, however, attempted to identify the signature of sausage oscillations via the indirect detection of intensity oscillations, e.g using Doppler shifts (Taroyan et al., 2007; Erdélyi & Taroyan, 2008) or periodicities in x-ray emission (e.g. Nakariakov et al., 2003) in the solar corona. To our knowledge, the first reported periodic oscillations in pore size were by Dorotovič et al. (2008), who observed periods from 20 minutes to 70 minutes in a photospheric pore with the Swedish Solar Telescope (SST). However, no intensity information was provided.

We present here observations of sausage oscillations in a pore detected using the Rapid Oscillations in the Solar Atmosphere (ROSA) instrument. The observations are in both pore size and intensity in the best cases and solely in pore size in other cases. The periods of the oscillations range between 50 s and 600 s and do not have constant frequency suggesting continual evolution of the pore due to dynamic behavior.

## 2. Observations and Data Reduction

One new and exciting ground-based setup is the ROSA instrument which provides high spatial (100 km, 2-pixel) and temporal (0.03 s) resolutions. ROSA is situated at the Dunn Solar Telescope and further details of the experimental setup and operation of ROSA are given in Jess et al. (2010). ROSA is able to observe at multiple wavelengths allowing the investigation of the magnetic connection between the various layers of the lower solar atmosphere from deep photosphere to the upper chromosphere.

### 2.1. Data

The data used here was taken by ROSA at 15 : 24 UT on the 22 August 2008. A group of 5 magnetic pores, shown in Fig. 1, were observed continually by ROSA for around 1 hr and 7 mins with a 50 Å wide filter centered at 4170 Å. The pores were formed before the observations began and all are still present in the final image of the observing run. The 4170 Å blue continuum filter samples the lower photosphere. The spatial sampling is 0.069" per pixel, giving a 2-pixel spatial

resolution of 0.138" (or 100 km) with an overall field of view of $50200 \times 50100$ km$^2$. The cadence obtained for this filter during the ROSA observing sequence was 0.2 s. The initial observations were processed through the ROSA data reduction pipeline which removed dark current, read-out noise, camera inconsistencies and variable light levels across the incident beam. To improve image quality the speckle reconstruction method was used with a ratio of 64 : 1. After processing, the cadence of the observations was reduced to 12.8 s. Intensities are normalised to the mean background value.

## 2.2. Analysis

The pores are observed close to disk center, and assuming that a pore is a waveguide which extends upwards into the solar atmosphere with a base in the photosphere, the line of sight is near perpendicular to the cross-section of the waveguide. This is ideal when searching for the periodic fluctuation in the area of the cross section. Images of the pore show it is distinctly non-circular in cross-section and movies of the magnetic pore reveal that it is highly dynamic. At present, there is no such theory describing waveguides with a complicated, non-symmetric geometry and dynamic behavior. Waves in more complicated models should still retain the same basic properties (see, e.g. Ruderman, 2003) so the approximation of a circular cross-section provides an adequate representation of the pore. The periodic change in the area of the cross-section is also accompanied by a periodic variation in intensity, which should be 180 degrees out of phase with the change in cross-sectional area for the sausage mode.

The method used for obtaining the pore size is as follows. Firstly we find the median value and variance of the intensity of the whole field of view in each frame. A 'box' is placed around each of the pores, large enough that the pore is contained within the box at all times. The area of the pore is then defined as being the number of pixels with a value of intensity $3\sigma$ less than the median value of intensity, providing a 99% confidence level that the dark pore pixels are contoured.

The data representing the size of the pore is then analysed using Empirical Mode Decomposition (EMD). This is a powerful tool that is capable of resolving non-stationary and non-linear time series. The theory is described in Huang et al. (1998) with excellent examples of applications to solar phenomena given in Terradas et al. (2004). EMD can overcome some of the problems associated with other analysis methods (e.g. wavelet analysis) and is suitable to decompose the time series into a finite number of Intrinsic Mode Functions (IMFs). The IMFs represent the different timescales of variations in the original times series. To determine whether a sausage oscillation is present, a direct comparison between IMFs of intensity and pore size with similar timescales is performed. This shows clearly out of phase behavior. A distinct sign of sausage oscillations is when periodic phenomena in cross-section and intensity are almost 180 degrees out of phase.

We shall refer to such a signal as a *strong* signal. Another, although not quite as distinct, signal is when periodicities in pore size do not match with any intensity variations. In such a case we can only assume the expected 'out of phase' intensity signal has been hidden by another effect that modifies the intensity. This will be referred to a *weak* signal in the following analysis. All signals will also have to be longer than $\sqrt{2}P$ to be considered as a real oscillation. The phase information is important for finding out of phase intensity and pore size oscillations. Unless comparisons can be made between the individual time series of intensity and pore size to compare the phases, then it is virtually impossible to identify whether the periodic oscillations in pore size are due to background intensity changes or the sausage mode. The EMD method allows an inspection of the different time-scales associated with the initial time-series and proves an ideal tool for analysis. We, however, apply the wavelet method to produce phase diagrams and compare to EMD results as control.

## 3. Oscillations in pores

The pore under consideration is located in the dashed box centered at $(15, 48)$ arcsecs in Fig. 1. The area is calculated with a confidence value of $3\sigma$, i.e 99% confidence. The average size of the pore is 536 pixels, which is roughly $1.36 \times 10^6$ km$^2$.

The IMFs are found for the average intensity per unit area and pore size time series and both time series reduce to 8 IMF components plus the trend. The IMFs have approximate characteristic periods $< 100$ s, 100 s, 150 s, 250 s, 400 s for IMFs $c_1$ to $c_5$. They have also been compared to wavelet plots of the two time series and the IMF components have periods that agree well with the periods that have significant power in the wavelets.

Table 1:: Periods of identified oscillations

| IMF | Strength | Period (s) | Start time (s) | Duration (s) |
|-----|----------|------------|----------------|--------------|
| $c_1$ | Strong | $30 \pm 13$ | 1200 | 100 |
| $c_2$ | Weak | $102 \pm 30$ | 1900 | 800 |
| $c_3$ | Weak | $140 \pm 13$ | 1700 | 400 |
| | Strong | $134 \pm 13$ | 2100 | 250 |
| | Weak | $126 \pm 40$ | 2350 | 1800 |
| $c_4$ | Weak | $180 \pm 13$ | 0 | 375 |
| | Weak | $281 \pm 18$ | 1700 | 750 |
| $c_5$ | Weak | $447 \pm 13$ | 1600 | 1350 |

In Fig. 2 (top panels) we show a comparison between the IMF components $c_1$ and $c_2$ of pore size (red dashed lines) and average intensity per unit area (solid black lines) for a small section of the time series. Fig. 2 also shows a comparison of the $c_3$, $c_4$ and $c_5$ components of intensity and pore size for the entire time series. The different oscillatory signals found are summarised in Table. 1. The oscillations here have an amplitude of $20 - 60$ pixels which corresponds to a $5 \times 10^4 - 1.5 \times 10^5$ km$^2$ increase in area, which is around $4 - 12\%$ of the average pore area. The small amplitude of the oscillation suggests that the sausage waves are linear in nature. To confirm the evidence for the sausage oscillations found in the comparison of the IMF components, we compare the two times series using cross wavelet analysis (see, e.g. Grinsted et al., 2004). We calculate the phase difference of the two time series in Fig. 2 (bottom right panel). It can be seen that the areas showing the strongest out of phase behavior correspond to the periods and events identified in the IMFs.

## 4. Which Mode

When it comes to determining which mode each period in Table 1 corresponds to, i.e. fast or slow, we require more information. This is due to the plasma-$\beta$ being close to 1 and the periods of the fast/slow modes are not as distinct as, say, in the corona. Due to the lack of velocity information we are also unable to determine whether the observed oscillatory signatures are standing or propagating modes. Assuming the pore is a straight, finite flux tube with a *uniform cross-section* situated between the photosphere and the transition region, then standing modes can be set up with the transition region acting as a reflector (see, e.g. Malins & Erdélyi, 2007). We can use the periods obtained from the EMD analysis to estimate the length of the waveguide that supports these oscillations. Typical values for pores are $T = 4000$ K, $B = 2$ kG, $\rho = 10^{-8} - 10^{-7}$ gcm$^{-3}$. These give values of $v_A = B/\sqrt{(\mu_0 \rho)} = 17 - 56$ kms$^{-1}$ and $c_s = \sqrt{(\gamma T/\tilde{\mu})} = 9$ kms$^{-1}$ where $\mu_0 = 4\pi$, $\gamma = 5/3$ and $\tilde{\mu} = 0.6$. The phase speed of the slow mode is close to the tube speed which has estimated value, $c_T = 8 - 9$ kms$^{-1}$. The fundamental period is given by $P \approx 2L/c_{ph}$ where $L$ is the tube length. Assuming the fundamental period is given by the oscillation identified in the $c_5$ IMF, which is $447 \pm 13$ s the length of the tube is then calculated to be $1.9 - 2.1$ Mm. If we now take the oscillation identified in the $c_4$ IMF, which has period of 180 s, and assume it is due to be the fast mode, we obtain $L = 1.5 - 5.0$ Mm for $c_{ph} = v_A = 17 - 56$ kms$^{-1}$. Both these estimates can provide a tube length which is comparable to the widely accepted and commonly used height of the transition region above the solar surface, i.e. required tube length to set up standing mode oscillations, which is around $\sim 2$ Mm. Note, this is not full proof of the nature of the observed oscillations. If future observations can identify the standing modes, then this should help in fast/slow mode identification.

A comment should be made here: the assumption that the tube is straight is a highly ideal assumption. The cross-section of the flux tube is actually expected to be expanding with height. Also, gravitational stratification plays a significant role in determining the density structuring in flux tubes located the photosphere and should also be taken into account (Luna-Cardozo et al., 2010).

## 5. Discussion

Observational evidence has been provided for examples of sausage oscillations in magnetic pores with a range of periods from ∼ 50 to ∼ 600 s. To our knowledge, this is only the second reported observation of oscillatory behavior in the area of a magnetic waveguide after Dorotovič et al. (2008). However, here we have a higher cadence allowing wave phenomena occurring on much shorter time-scales to be resolved. Our observations also provide intensity information about the interior plasma of the pore, where oscillatory behavior is also seen.

The oscillatory phenomena were identified using a relatively new technique (at least to solar applications) known as Empirical Mode Decomposition. Direct comparison between intensity IMFs and pore size IMFs allowed the identification of out of phase oscillatory signatures, indicating the presence of sausage oscillations. This was supported by calculation of the relative phase between the two time series. This method highlights the difficulties in obtaining a clear signal of sausage oscillations by measuring the cross-sectional area of the waveguide. Periodic changes in pore size can be related to periodic behavior in intensity (i.e. in phase periodic behavior with similar power). Using a method like wavelet analysis alone would not allow the comparison of the phases of intensity and pore size without ambiguity. Hence, wavelet analysis alone could lead to false detections of sausage modes.

Only a few sections in the various IMFs provided a clear signal of sausage oscillations, were the oscillation in pore size and intensity in the pore are out of phase by 180 degrees. The other signals in Table 1 show oscillations in pore size that are not identified with a change in intensity, hence, are a somewhat weaker signal of sausage oscillation. The periodic phenomena in intensity can most likely be attributed to global acoustic modes which are omnipresent in the photosphere and are found both inside the pore and in the surrounding granules and have a wide range of periods from tens of second to tens of minutes (see, e.g. Jess et al., 2007).

Due to the omnipresent nature of the global acoustic oscillation in the surrounding granules, it is proposed the main driver for these oscillations is the global acoustic mode. The periods found mainly correspond to the 3 and 5 minute global modes that have been numerously reported, adding further strength to the argument. The question of whether the detected modes are standing or

propagating remains unanswered due to the lack of velocity data, which could have answered this. For example, the signals at $t = 1700$ s in $c_3$ and $c_4$ could correspond to different harmonics of the standing sausage oscillation. A plausible suggestion that the oscillations were standing modes led to the estimation of waveguide lengths that are comparable to the distance from the photosphere to the transition region, i.e. the two boundaries required to set up standing modes in the lower solar atmosphere.

## REFERENCES

Banerjee, D., Erdélyi, R., Oliver, R., & O'Shea, E. 2007, Sol. Phys., 246, 3

Bonet, J. A., Márquez, I., Sánchez Almeida, J., Cabello, I., & Domingo, V. 2008, ApJ, 687, L131

De Moortel, I. 2009, Spac. Sci. Rev., 149, 65

Dorotovič, I., Erdélyi, R., & Karlovský, V. 2008, in IAU Symposium, Vol. 247, IAU Symposium, eds. R. Erdélyi & C. A. Mendoza-Briceño, 351–354

Edwin, P. M. & Roberts, B. 1983, Sol. Phys., 88, 179

Erdélyi, R. & Fedun, V. 2010, Sol. Phys., 263, 63

Erdélyi, R. & Morton, R. J. 2009, A&A, 494, 295

Erdélyi, R. & Taroyan, Y. 2008, A&A, 489, L49

Evans, D. J. & Roberts, B. 1990, ApJ, 348, 346

Grinsted, A., Moore, J. C., & Jevrejeva, S. 2004, Nonlin. Pro. Geophys., 11, 561

Huang, N. E., Shen, Z., Long, S. R., et al. 1998, Royal Society of London Proceedings Series A, 454, 903

Jess, D. B., Andić, A., Mathioudakis, M., Bloomfield, D. S., & Keenan, F. P. 2007, A&A, 473, 943

Jess, D. B., Mathioudakis, M., Christian, D. J., et al. 2010, Sol. Phys., 261, 363

Jess, D. B., Mathioudakis, M., Erdélyi, R., et al. 2009, Science, 323, 1582

Klimchuk, J. A. 2006, Sol. Phys., 234, 41

Luna-Cardozo, M., Verth, G., & Erdélyi, R. 2010, A&A, Submitted

Malins, C. & Erdélyi, R. 2007, Sol. Phys., 246, 41

Mathioudakis, M., Jess, D. B., & Erdélyi, R. 2010, Spac. Sci. Rev., Submitted

Nakariakov, V. M., Melnikov, V. F., & Reznikova, V. E. 2003, A&A, 412, L7

Roberts, B. 1981, in The Physics of Sunspots, eds. L. E. Cram & J. H. Thomas, 369–383

Roberts, B. 1992, in NATO ASIC Proc. 375: Sunspots. Theory and Observations, eds. J. H. Thomas & N. O. Weiss, 303–331

Roberts, B. & Webb, A. R. 1978, Sol. Phys., 56, 5

Ruderman, M. S. 2003, A&A, 409, 287

Sankarasubramanian, K. & Rimmele, T. 2003, ApJ, 598, 689

Sobotka, M. 2003, Astronomische Nachrichten, 324, 369

Taroyan, Y. & Erdélyi, R. 2009, Spac. Sci. Rev., 149, 24

Taroyan, Y., Erdélyi, R., Wang, T. J., & Bradshaw, S. J. 2007, ApJ, 659, L173

Terradas, J., Oliver, R., & Ballester, J. L. 2004, ApJ, 614, 435

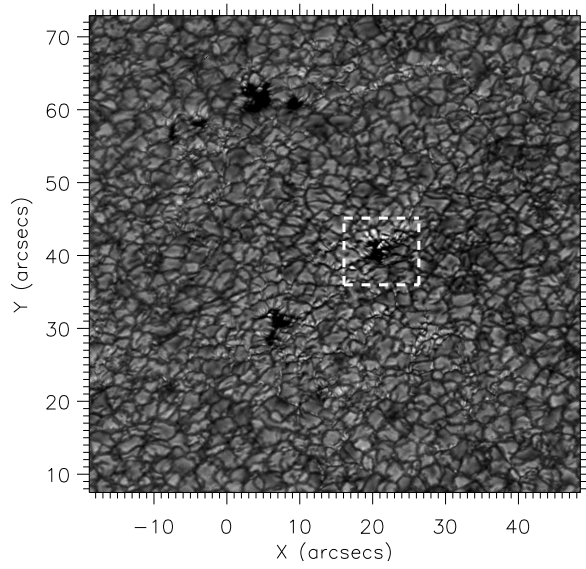Zaqarashvili, T. V. & Erdélyi, R. 2009, Spac. Sci. Rev., 149, 355

Fig. 1.—: Field of view observed by ROSA on 22 August 2008. Boxed areas highlight pore in which oscillations are present.
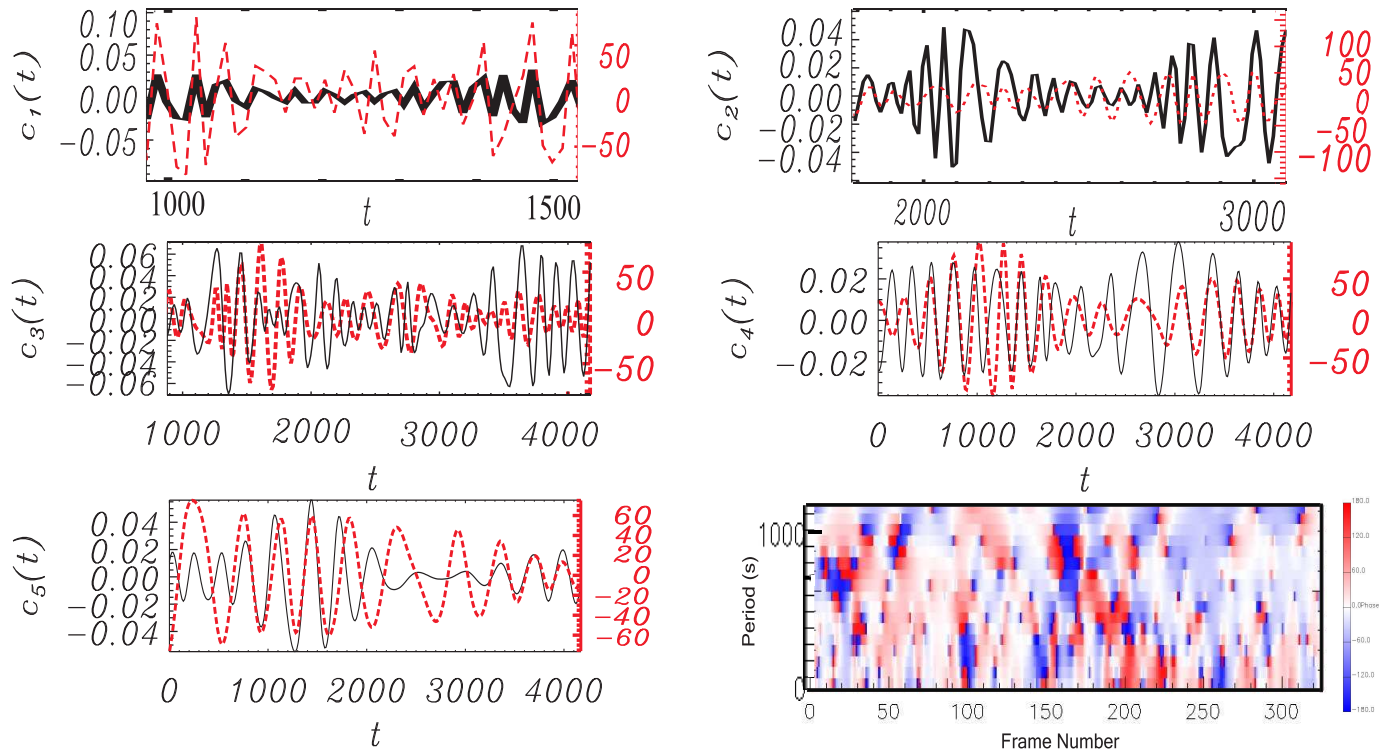
Fig. 2.—: Shown is a direct comparison between IMF components of intensity (black solid lines) and pore size (red dashed lines). The intensity is normalised with respect to the background mean value and the pore size is measured in pixels. Last panel shows wavelet phase plot for two the time series.